Talanta 81 (2010) 760–765

Contents lists available at ScienceDirect

Talanta

journal homepage: www.elsevier.com/locate/talanta

# Protein determination using methylene blue in a synchronous fluorescence technique

Xiaoyu Liu, Xia Wu*, Jinghe Yang

*Key Laboratory of Colloid and Interface Chemistry (Shandong University), Ministry of Education, School of Chemistry and Chemical Engineering, Shandong University, Jinan, Shandong Province 250100, PR China*

ARTICLE INFO

*Article history:*
Received 11 November 2009
Received in revised form 6 January 2010
Accepted 9 January 2010
Available online 18 January 2010

*Keywords:*
Methylene blue dimer
Protein
Synchronous fluorescence
Deaggregation

ABSTRACT

A new method for detecting protein by synchronous fluorescence enhancement was developed, based on the combination of near infrared (NIR) fluorescence and the dedimerization phenomenon of methylene blue (MB). Under analytical conditions, there are linear relationships between the enhancing extent of synchronous fluorescence of MB–sodium dodecyl benzene sulfonate (SDBS)–protein at 667 nm and the concentration of protein in the range of $8.0 \times 10^{-8}$–$4.0 \times 10^{-5}$ g mL$^{-1}$ for bovine serum albumin (BSA), $1.0 \times 10^{-7}$–$3.5 \times 10^{-5}$ g mL$^{-1}$ for egg albumin (EA). The detection limits (S/N = 3) of BSA and EA are 8.9 ng mL$^{-1}$ and 10.0 ng mL$^{-1}$, respectively. The fluorescence enhancement mechanism is discussed in detail. Results from multiple techniques indicate that the fluorescence enhancement of the system originates from the hydrophobic microenvironment provided by BSA and SDBS, and the formation of an MB–SDBS–BSA complex, as well as the deaggregation of some MB dimer.



## 1. Introduction

Determination of protein continues to be an important technique in life science applications. Some commonly used methods for the protein determination have disadvantages, such as low sensitivity and selectivity [1–3], and new techniques continue to be developed in many laboratories. Fluorimetric techniques [4] have been widely implemented recently due to their high sensitivity and selectivity. Proteins possessing Try or Trp residues exhibit natural fluorescence, but it is difficult to use natural fluorescence for analysis of proteins at low concentration, or for proteins lacking these residues. Thus, extrinsic fluorescence probes must be employed for the determination of dilute protein; a number of methods for the determination of proteins have been established based on such extrinsic fluorescence probes utilizing rare earth ions and their complexes, or by using fluorescence dyes and quantum dots [5–15]. Recently, analytical studies with fluorescence dyes have focused on both near infrared (NIR) fluorescence dyes [16,17] and the dimerization of fluorescent dyes [18] in solution. Typically, NIR fluorescent dyes emit in the region of 600–1000 nm, where most biomolecules have no absorption, and typically give rise to minor interference so that NIR techniques are especially suitable for studies of biological samples. Dimerization is a phenomenon of some dyes with planar structure that occurs not only in aqueous solution, but also in ionic surfactant solutions [19].

Methylene blue (MB) is a NIR fluorescent dye, which may be used as a photosensitizer, and shows promising applications in the area of photodynamic therapy [20]. Because it is a cationic molecule with planar structure, MB interacts easily with the biomacromolecules [21,22]. To our knowledge, MB acting as a probe for the determination of proteins based on its NIR fluorescence properties and its dimerization has not been reported.

In this study we found that MB can form the dimer in the presence of SDBS, resulting in fluorescence quenching of MB. However, the fluorescence intensity is greatly enhanced when proteins such as BSA or EA are added into the MB–SDBS system. Based on this phenomenon, a synchronous fluorescence technique (SFT) for protein determination was developed. SFT is necessary because the maximum excitation wavelength of MB (667 nm) is close to its emission wavelength (683 nm), where Rayleigh light scattering at 667 nm can interfere the fluorescence measurement. Synchronous fluorescence spectroscopy provides a simplified spectrum with sharp emission peaks, and because of its sharp and narrow spectrum, SFT is a good method for quantitative determinations [23]. Experimental results indicate that this method has the advantages of high sensitivity with detection limits at nanogram level, and has been applied to the determination of actual protein samples with satisfactory results. Finally,

* Corresponding author. Tel.: +86 531 88365459; fax: +86 531 88564464.
*E-mail address:* wux@sdu.edu.cn (X. Wu).

0039-9140/$ – see front matter © 2010 Elsevier B.V. All rights reserved.
doi:10.1016/j.talanta.2010.01.014

the mechanism of fluorescence enhancement in this system is discussed.

## 2. Experimental

### 2.1. Materials

Stock solutions of protein ($1.0 \times 10^{-3}$ g mL$^{-1}$) were prepared by dissolving commercial BSA (0.1000 g, Ameresco Co., USA) and EA (0.1000 g, Sigma, USA) in doubly distilled water and diluted to 100 mL, stored at 0–4 °C. A stock standard solution ($1.0 \times 10^{-3}$ mol L$^{-1}$) of MB (Tianjin Beihong Chemical Co., China) was prepared by dissolving 0.0380 g MB in doubly distilled water and diluting to 100 mL. A solution made up of 0.8710 g SDBS (BBI, Canada) was prepared ($1.0 \times 10^{-2}$ mol L$^{-1}$) in doubly distilled water and diluted to 250 mL. Hexamethylenetetramine (HMTA)–HCl buffer solution was prepared by dissolving HMTA (10.0 g) in 90 mL water and adjusting the pH to 6.80 with HCl ($1.0 \times 10^{-1}$ mol L$^{-1}$). All reagents and solvents were analytical grade unless otherwise noted, and used as received.

### 2.2. Apparatus

Synchronous fluorescence spectra, resonance light scattering spectra and fluorescence polarization were recorded with Perkin-Elmer LS-55 spectrofluorimeter in a 1 cm quartz cuvette. Absorption spectra were measured on a U-4100 spectrophotometer (Hitachi, Japan). Solution surface tension was measured on a Processer Tensionmeter-K12 (Krüss Corp., German). pH was measured on a Delta 320-S pH meter (Mettler-Toledo, Shanghai). Zeta potentials ($\zeta$) were measured with a JS94H micro-television electrophoretic instrument (ZhongChen Co., China). The Far-UV CD spectra were measured on a JASCO J-810 Circular Dichroism Chiroptical Spectrophotometer (Japan).

### 2.3. Method

To a 25 mL test tube, solutions were added in the following order: HMTA–HCl, MB, SDBS, BSA. The mixture was thoroughly mixed and diluted to 10 mL with water, and its synchronous fluorescence was measured at $\lambda = 667$ nm ($\Delta\lambda = 15$ nm). The extent of synchronous fluorescence enhancement is defined as $\Delta I_f = I_f - I_0$, where $I_f$ and $I_0$ are the fluorescence intensities of the solution with and without protein, respectively.

## 3. Results and discussion

### 3.1. Fluorescence spectra

Fig. 1 shows the emission and synchronous fluorescence spectra of the components and solutions developed in this study. As can be seen in Fig. 1(a), the characteristic fluorescent peak of MB is observed at 683 nm when using an excitation wavelength of 667 nm. The interference of Rayleigh light scattering (667 nm) is obvious. To avoid this interference, a synchronous fluorescence scan was used for the fluorescence measurement. Fig. 1(b) illustrates the synchronous fluorescence peaks of MB, MB–SDBS, MB–SDBS–BSA solutions at 667 nm with a $\Delta\lambda$ of 15 nm; this value for $\Delta\lambda$ was selected for further determinations. Fig. 1(b) also indicates that the synchronous fluorescence intensity of MB is quenched by SDBS, but after addition of protein (such as BSA, etc.), the fluorescence intensity of the system is enhanced. The increased fluorescence intensity at 667 nm is proportional to the concentration of protein, and the system of MB–SDBS–BSA was chosen for further quantitative study.

### 3.2. Effect of pH and buffer

The effect of pH and buffer was studied. The maximum $\Delta I_f$ occurred at pH = 6.80. The effects of different buffers on the $\Delta I_f$ (%) of the system were also tested at the same pH (pH = 6.80 ± 0.1). The $\Delta I_f$ (%) for HMTA–HCl, Tris–HCl, Britton–Robinson, water, and $KH_2PO_4$–$Na_2HPO_4$ are 100, 64.8, 23.1, 75.6 and 23.5, respectively. The results indicated that the type of buffers has a large effect on the system, and HMTA–HCl (pH = 6.80, 0.5 mL) was selected as the most suitable buffer for this study.

### 3.3. Effect of MB concentration

To determine an optimal concentration for MB in the analytical method, the fluorescence intensities as a function of MB concentration were determined. The value for $\Delta I_f$ reached a maximum at approximately $1.4 \times 10^{-6}$ mol L$^{-1}$, and was subsequently used for further studies.

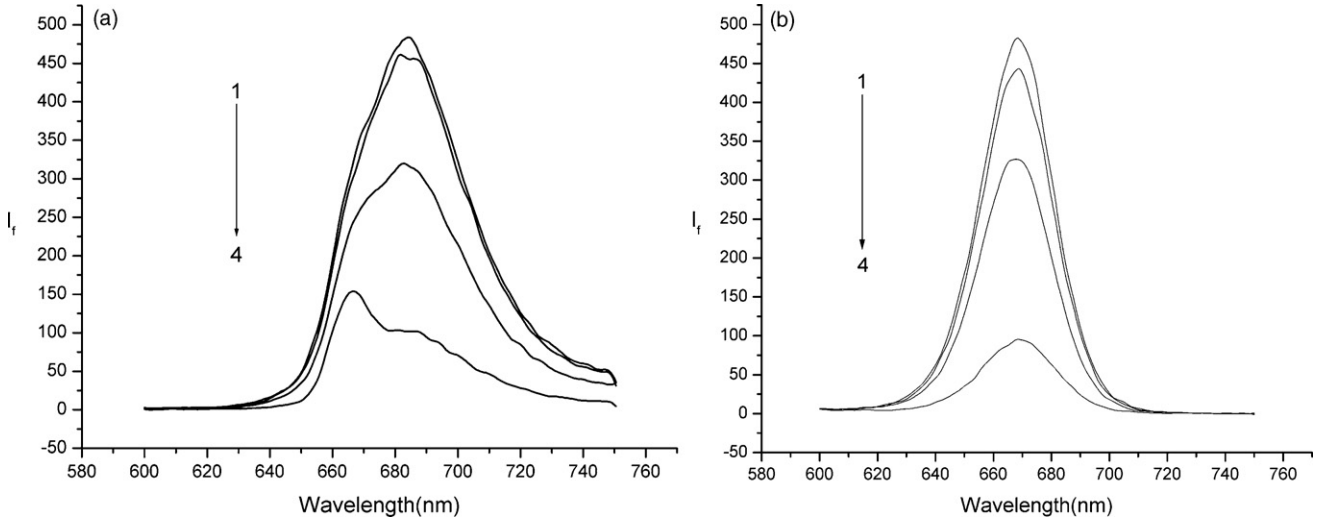


**Fig. 1.** Emission spectra (a) and synchronous fluorescence spectra (b): (1) MB; (2) MB–BSA; (3) MB–SDBS–BSA; (4) MB–SDBS. Conditions: HMTA: 1.0% (pH = 6.80); MB: $1.4 \times 10^{-6}$ mol L$^{-1}$; SDBS: $1.2 \times 10^{-4}$ mol L$^{-1}$; BSA: $1.0 \times 10^{-5}$ g mL$^{-1}$.

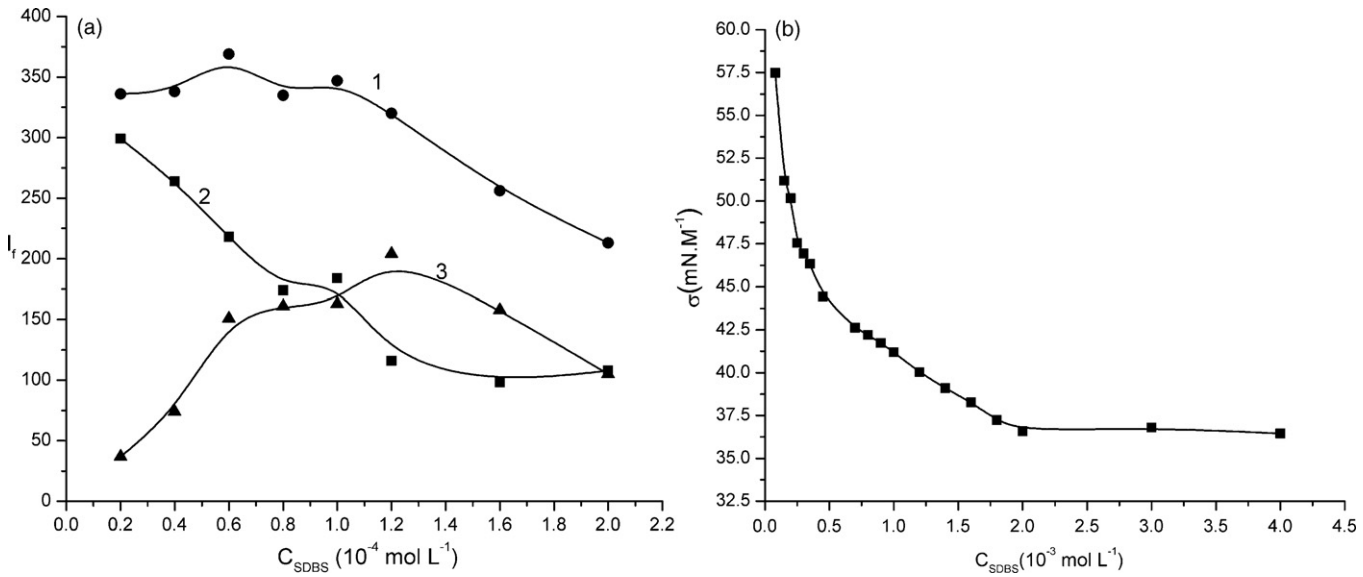


**Fig. 2.** (a) Effect of SDBS. 1: $I_f$; 2: $I_0$; 3: $\Delta I_f$. Conditions: HMTA: 1.0% (pH = 6.80); MB: $1.4 \times 10^{-6}$ mol $L^{-1}$; BSA: $1.0 \times 10^{-5}$ g $mL^{-1}$. (b) The surface tension of the system. Conditions: HMTA: 1.0% (pH = 6.80); MB: $1.4 \times 10^{-6}$ mol $L^{-1}$; BSA: $1.0 \times 10^{-5}$ g $mL^{-1}$.

### 3.4. Effect of surfactants

The synchronous fluorescence intensity was measured in the presence of surfactants. The $\Delta I_f$ for SDBS, sodium dodecylsulfonate, sodium lauryl sulfate, cetylpyridinium bromide, cetyltrimethylammonium bromide, and Emulsifier OP are 100, 82, 14, 3, 10 and 5, respectively, and related as the % of the value obtained for SDBS. Since the addition of SDBS led to the greatest difference in fluorescence, the effect of SDBS was studied as a function of its concentration (Fig. 2(a)); from the data, a value of $1.2 \times 10^{-4}$ mol $L^{-1}$ was chosen for further studies.

Fig. 2(b) illustrates the surface tension of the SDBS in this system. The critical micelle concentration (CMC) of SDBS in this system is $1.8 \times 10^{-3}$ mol $L^{-1}$, which is higher than the optimum concentration of SDBS ($1.2 \times 10^{4}$ mol $L^{-1}$) in this experiment. So, it is considered that SDBS exists as the pre-micelle or single molecule in the studied system.

### 3.5. The addition order and stability of the system

In practice, the best order of addition of the reagents was found to be HMTA–HCl, MB, SDBS and protein. Under the optimized concentration and buffer conditions, the effect of incubation time on the synchronous fluorescence intensity was also studied. The value of $\Delta I_f$ reaches a maximum at approximately 20 min after all reagents had been added and remained stable for at least 2.0 h.

### 3.6. Interfering species

Under the analytical conditions, various standard reagents were examined for their interference of the fluorescence of the MB–SDBS–protein mixture (Table 1). Most amino acids and metal ions, except $Fe^{3+}$, $Fe^{2+}$ and $Al^{3+}$, had no or little effect on the determination of BSA at ±5% relative error.

## 4. Analytical application

### 4.1. Calibration curve and detection limits

Under optimized conditions, the analytical parameters of this method are listed in Table 2. It shows that there is a good linear relationship between $\Delta I_f$ and the concentrations of BSA and EA. And their limits of detection reached at nanogram levels, according to the relation $k \times S_0/N$ (where $k = 3$ for LOD, $k = 10$ for LOQ, $S_0$ is the standard deviation of the blank and $N$ is the slope of the calibration curve).

### 4.2. Determination of actual sample

The method of standard addition was used for the determination of EA in actual sample. The egg albumin from eggs without any further purification was diluted into 1000 times for protein determination. In the UV spectrophotometric method, here used as a comparative analytical technique, the above EA actual sample of the same volume was diluted into 10 times and the near-UV absorbance at 280 nm was used to quantify the EA concentration. The results are compared in Table 3.

**Table 1**
Interfering species.

| Foreign substance | Concentration coexisting ($\times 10^{-6}$ mol $L^{-1}$) | Change of $\Delta I_f$ (%) |
|---|---|---|
| $K^+$, $Cl^-$ | 25 | −3.9 |
| $Ca^{2+}$, $Cl^-$ | 15 | −4.2 |
| $Al^{3+}$, $NO_3^-$ | 0.5 | 5.0 |
| $NH_4^+$, $Cl^-$ | 3.5 | 3.7 |
| $Na^+$, $SO_4^{2-}$ | 8.0 | −4.6 |
| $Ba^{2+}$, $Cl^-$ | 6.0 | −4.2 |
| $Na^+$, $Cl^-$ | 40 | −4.9 |
| $Mg^{2+}$, $SO_4^{2-}$ | 20 | 5.1 |
| $Zn^{2+}$, $Cl^-$ | 4.0 | 4.1 |
| $Na^+$, $CO_3^{2-}$ | 15 | −4.9 |
| $Fe^{3+}$, $Cl^-$ | 0.3 | −4.5 |
| $Fe^{2+}$, $SO_4^{2-}$ | 0.4 | −5.1 |
| L-Asp | 75 | −4.1 |
| L-His | 70 | −3.4 |
| L-Phe | 15 | 3.9 |
| Cys | 10 | −3.5 |
| DL-Glu | 80 | −3.5 |
| DL-Thr | 60 | −5.1 |
| yRNA | 50 (μg $mL^{-1}$) | 4.5 |
| fsDNA | 45 (μg $mL^{-1}$) | 4.6 |
| ctDNA | 65 (μg $mL^{-1}$) | 4.4 |

Conditions: MB: $1.4 \times 10^{-6}$ mol $L^{-1}$; SDBS: $1.2 \times 10^{-4}$ mol $L^{-1}$; BSA: $5.0 \times 10^{-7}$ g $mL^{-1}$; HMTA: 1.0% (pH = 6.80).

**Table 2**
Analytical parameters of this method.

| Proteins | Linear range ($\mu g\,mL^{-1}$) | Linear regression equation ($g\,mL^{-1}$, $n=3$) | $r^a$ | LOD[b] ($ng\,mL^{-1}$) | LOQ[c] ($\times10^{-8}\,g\,mL^{-1}$) |
|---|---|---|---|---|---|
| BSA | 0.080–40.0 | $\Delta I = 103.8 + 1.98 \times 10^7 C$ | 0.998 | 8.9 | 3.0 |
| EA | 0.100–35.0 | $\Delta I = 99.5 + 1.88 \times 10^7 C$ | 0.997 | 10 | 3.3 |

[a] Correlation coefficient.
[b] Limit of detection.
[c] Limit of quantification.

**Table 3**
The results of samples determination.

| Samples | Methods | Concentration ($mg\,mL^{-1}$) | Average ($mg\,mL^{-1}$) | RSD (%) |
|---|---|---|---|---|
| EA | Proposed method | 100.9, 100.8, 101.2, 97.7, 101.1 | 100.3 | 1.5 |
| | UV method | 100.6, 101.6, 97.6, 98.2, 99.2 | 99.4 | 1.7 |

RSD, relative standard deviation.

## 5. Mechanism of the interaction among MB, SDBS and BSA

### 5.1. The formation of MB dimer

MB is a cationic heterocyclic aromatic molecule; its behavior at different concentrations [24] can be interpreted by the changes in solution absorption and synchronous fluorescence spectra, as shown in Fig. 3. With increasing concentration of MB, the absorption peaks at 664 nm blue shifts to 661 nm, and the intensity of absorption peaks at 610 nm increases; concomitantly, the $\beta$ ratios ($\beta = A_{661}/A_{610}$) decrease. From the synchronous fluorescence spectra, the larger the concentration of MB leads to a stronger fluorescence intensity at 667 nm, but the intensity decreases when the concentration of MB is larger than $1.0 \times 10^{-5}$ mol $L^{-1}$, and exhibits a 'red-shift'. The above phenomena are taken to show that MB in high concentration forms a donor/acceptor dimer complex [25].

In the structure of MB, the dimethyl amine and ammonium groups are the electronic donor and acceptor, respectively, linked via a heterocyclic aromatic core. Thus MB is a D-π-A molecule that possesses HOMO and LUMO energy levels that are close in energy; its first excited state is an intramolecular charge transfer (ICT), which allows its dipole moment to be much larger than that of ground state. At higher concentration of MB, the ICT is enhanced via intermolecular interactions, resulting in the formation of $D^+$-π-A and D-π-$A^-$ or $D^+$-π-$A^-$ state, which induces the blue-shift of the absorption peak and the red-shift of the synchronous fluorescence peak of MB. All of the phenomena above indicate that the aggregation of MB belongs to a kind of H-aggregation [26,27].

The selected analytical concentration of MB is $1.4 \times 10^{-6}$ mol $L^{-1}$, where MB is expected to exist as a monomer. However, when SDBS is added to the MB solution, the intensity of absorption at 661 nm decreases (Fig. 4), and a higher concentration of SDBS leads to lower $\beta$ ratios ($\beta = A_{661}/A_{610}$). This indicates that SDBS promotes the formation of MB dimer, since the concentration of SDBS is below its CMC and the surfactant is in a pre-micellar form. At the same time, water molecules may form a regular region around the surfactant molecules or pre-micelles, termed an "iceberg structure", which also may help stabilize MB dimerization [28].

### 5.2. The deaggregation of MB dimer and the formation of MB–SDBS–BSA

From the absorption spectra shown in Fig. 5, it can be seen that the peak of 661 nm decreases when BSA is added into MB, but the peak of 610 nm has little change. In contrast SDBS addition leads to an increase in absorption at 610 nm along with the decrease at 661 nm. Overall, when BSA is added into MB–SDBS, it can be seen that $\beta_{MB} > \beta_{MB-BSA} > \beta_{MB-SDBS-BSA} > \beta_{MB-SDBS}$. The result indicates that BSA inhibits the formation of MB dimer, resulting in a partial

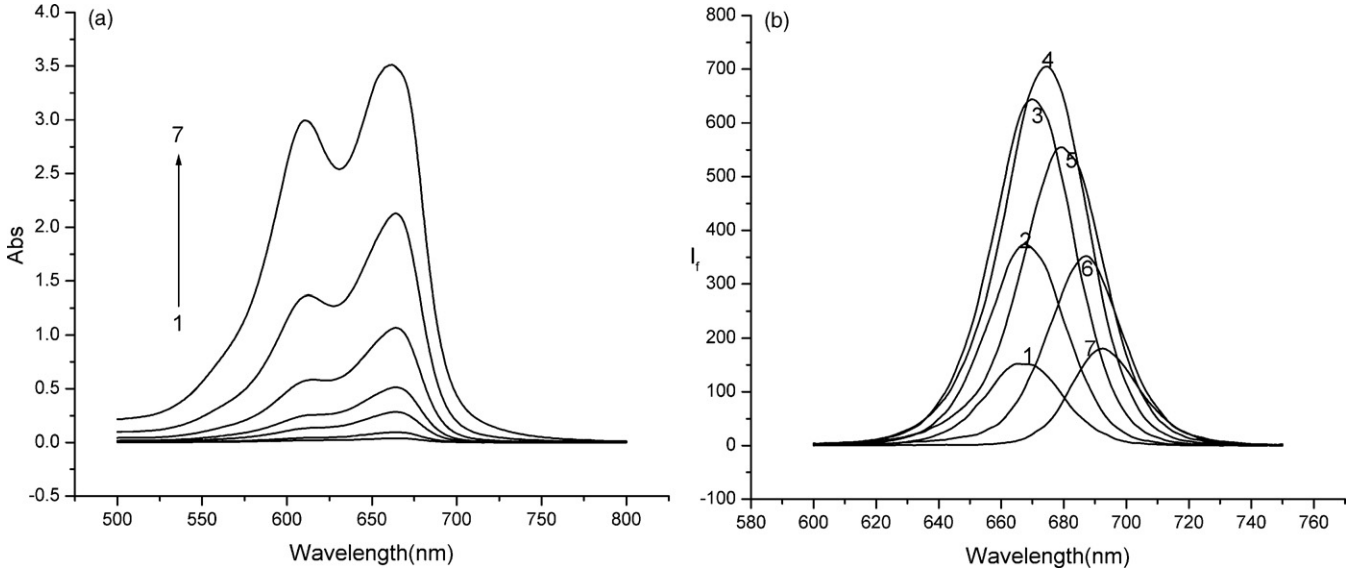


**Fig. 3.** The aggregation of MB. (a) The absorption spectra of MB. (b) The synchronous fluorescence spectra of MB. (1–7) The concentrations of MB are $8.0 \times 10^{-7}$, $2.0 \times 10^{-6}$, $5.0 \times 10^{-6}$, $1.0 \times 10^{-5}$, $2.0 \times 10^{-5}$, $4.0 \times 10^{-5}$ and $8.0 \times 10^{-5}$ mol $L^{-1}$, respectively. Conditions: HMTA: 1.0% (pH = 6.80).

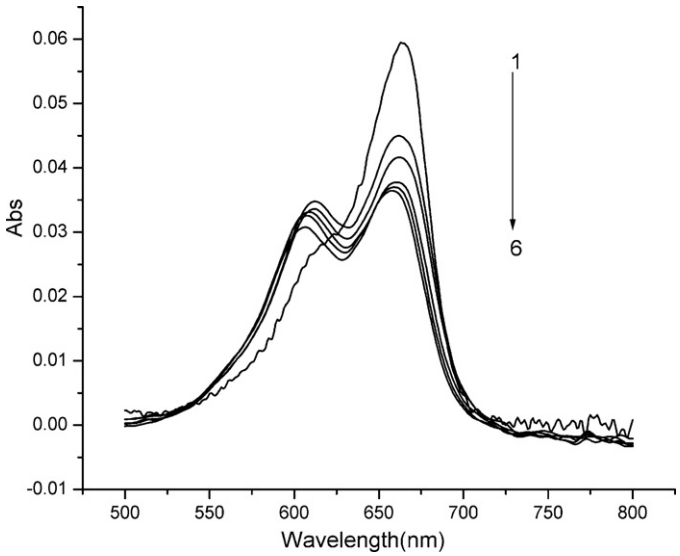


**Fig. 4.** Absorption spectra of MB and SDBS. (1–6) The concentrations of SDBS are 0.0, $6.0 \times 10^{-5}$, $8.0 \times 10^{-5}$, $1.0 \times 10^{-4}$, $1.2 \times 10^{-4}$ and $1.4 \times 10^{-4}$ mol $L^{-1}$, respectively. Conditions: HMTA: 1.0% (pH = 6.80); MB: $1.4 \times 10^{-6}$ mol $L^{-1}$.

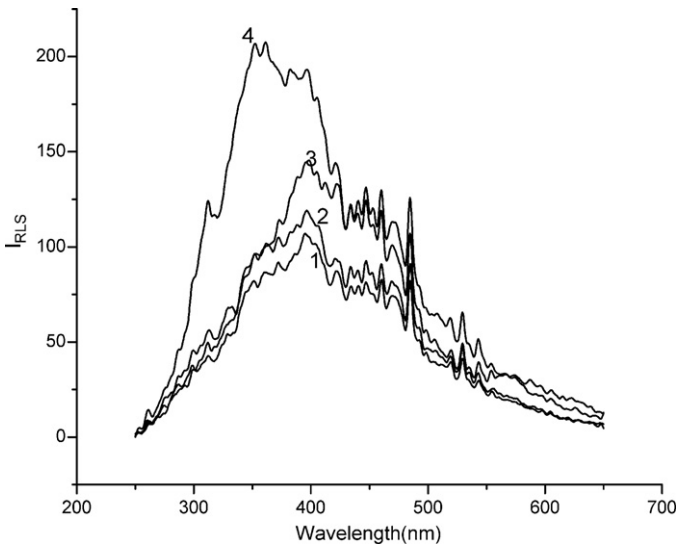


**Fig. 6.** Resonance light scattering spectra of the system. (1) MB; (2) MB–SDBS; (3) MB–BSA; (4) MB–SDBS–BSA. Conditions: HMTA: 1.0% (pH = 6.80); MB: $1.4 \times 10^{-6}$ mol $L^{-1}$; SDBS: $1.2 \times 10^{-4}$ mol $L^{-1}$; BSA: $1.0 \times 10^{-5}$ g $mL^{-1}$.

deaggregation of the dimer because of the formation of BSA–SDBS negative complex and the binding of BSA and MB. At the same time, the positive MB dimer can dissolve into the negative SDBS–BSA cluster through electrostatic and hydrophobic forces and a strong association is formed among BSA, SDBS and MB dimer. This result can also be confirmed by resonance light scattering (RLS) spectra (Fig. 6), that indicates that the resonance light scattering intensity of the MB–SDBS–BSA solution is maximized, which is taken to indicate that a large complex is present [29].

The zeta potential ($\xi$) of the analytical system with different concentrations of MB was assessed (Fig. 7). It can be seen that the $\xi$ of SDBS and BSA is initially −14.66 mV; with addition of MB, the $\xi$ increased and reached positive values. Thus, in MB–SDBS–BSA system, SDBS–BSA (negative charge) and MB (positive charge) form a large complex (MB–SDBS–BSA).

### 5.3. Secondary structural change of BSA

Circular dichroism (CD) spectra of proteins provide important qualitative information about expected secondary structural changes, due to interactions between protein molecules or between protein and exogenous molecules. A double-negative peak in the CD spectra is an indication of α-helical secondary structure. The peak at 220 nm is the contribution of the n–π* transition of peptide bond, and the peak at 208–209 nm is due to the π–π* transition of peptide bond [30]. CD spectra (Fig. 8) were analyzed using the Chen–Yang principle to obtain structural information due to changes in the analytical conditions. The changes of α-helix, β-sheet, β-turn and random coil in BSA under the analytical conditions are shown in Table 4. In general, all of the four structures of BSA changed with the addition of SDBS, MB and MB–SDBS, which indicates that there is a strong interaction among MB, SDBS and BSA.

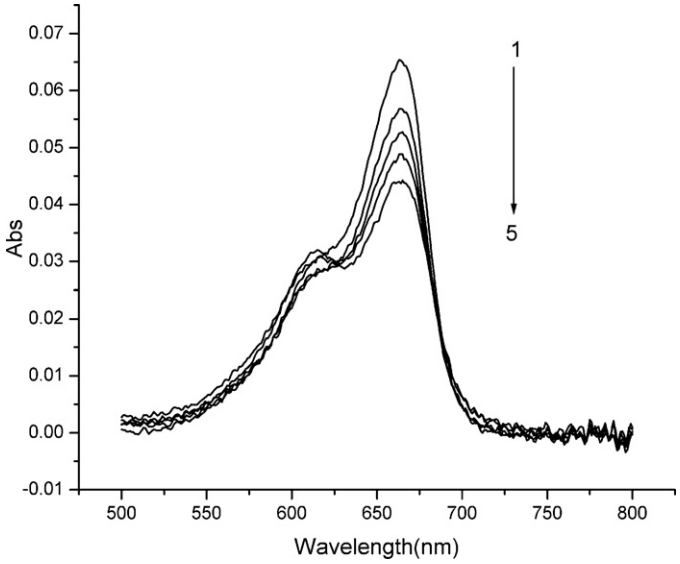


**Fig. 5.** Absorption spectra of the system. (1) MB; (2) BSA–MB; (3) MB–SDBS–BSA ($1.0 \times 10^{-5}$ g $mL^{-1}$); (4) MB–SDBS–BSA ($5.0 \times 10^{-6}$ mol $L^{-1}$); (5) MB–SDBS. Conditions: HMTA: 1.0% (pH = 6.80); MB: $1.4 \times 10^{-6}$ mol $L^{-1}$; SDBS: $1.2 \times 10^{-4}$ mol $L^{-1}$.

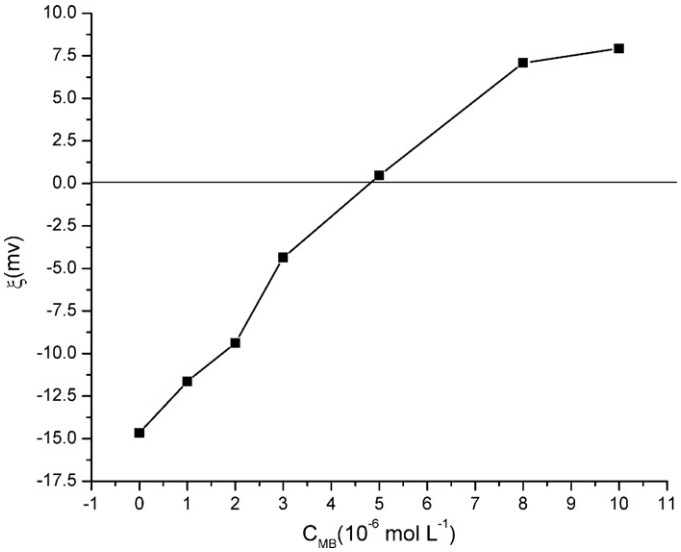


**Fig. 7.** The $\xi$ of the system. Conditions: HMTA: 1.0% (pH = 6.80); SDBS: $1.2 \times 10^{-4}$ mol $L^{-1}$; BSA: $6.0 \times 10^{-4}$ g $mL^{-1}$.

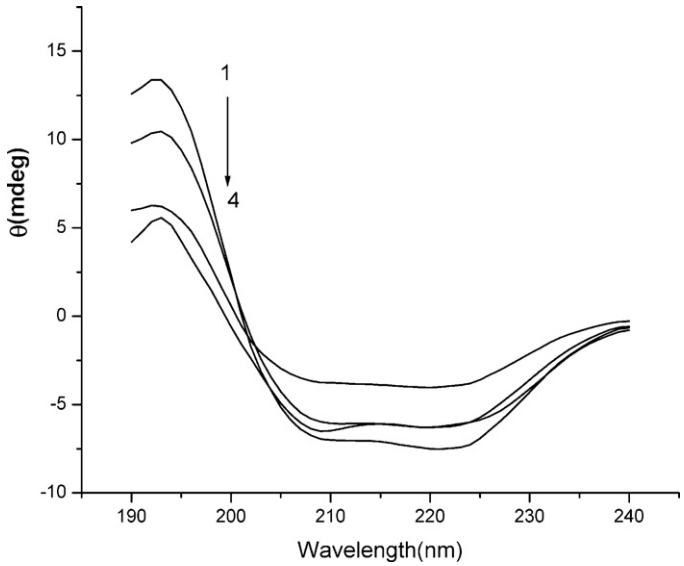


**Fig. 8.** The far-UV CD spectra of the system. (1) BSA; (2) BSA–MB; (3) BSA–SDBS; (4) MB–SDBS–BSA. Conditions: HMTA: 1.0% (pH = 6.80); MB: $1.4 \times 10^{-6}$ mol $L^{-1}$; SDBS: $1.2 \times 10^{-4}$ mol $L^{-1}$; BSA: $1.0 \times 10^{-5}$ g $mL^{-1}$.

**Table 4**
Comparison of BSA secondary structure in the presence of different components.

| | α-Helix (%) | β-Sheet (%) | β-Turn (%) | Random (%) |
|---|---|---|---|---|
| BSA | 34.7 | 38.1 | 1.2 | 26.0 |
| BSA–MB | 33.1 | 36.3 | 5.0 | 25.6 |
| BSA–SDBS | 27.2 | 16.3 | 19.9 | 36.7 |
| BSA–MB–SDBS | 30.2 | 42.9 | 0.1 | 26.8 |

### *5.4. The microenvironment of the system*

Finally, the microenvironment of the systems was assessed using the technique that compares the ratios of the first to third fluorescence bands of pyrene monomer ($I_1/I_3$) in the solution as function of probe which reflects polarity changes experienced by the pyrene [31,32]. A high value reflects a less hydrophobic environment. The ratios of the first to third fluorescence bands of pyrene monomer in buffer, SDBS, BSA and SDBS–BSA are 1.690, 1.663, 1.640, and 1.315. The result indicates that the hydrophobicity of MB system increases with added SDBS and BSA, corresponding to the enhancement of the synchronous fluorescence intensity of MB–SDBS complex.

According to the Perrin equation, the microviscosity of the microenvironment can be estimated using the fluorescence anisotropy of a fluorescence probe [33]; a large value reflects a larger microviscosity. The polarization values of MB in buffer, SDBS, BSA and SDBS–BSA media were 0.053, 0.132, 0.143 and 0.209, respectively, indicating that the BSA–SDBS system provides a maximum microviscosity for MB, also enhancing the maximum fluorescence intensity of MB–SDBS–BSA complex.

Based on the above observations, the BSA–SDBS system provides an optimum hydrophobic and viscous environment for MB, which leads to the enhanced synchronous fluorescence intensity. In addition, the hydrophobic environment of BSA–SDBS system also prevents collisions between the protein complex and water to decrease the energy losses in the MB–SDBS–BSA system.

## 6. Conclusion

In conclusion, the combination of MB NIR fluorescence, its dimerization phenomenon, and a synchronous fluorescence technique has been developed into a method for protein determination. This method shows potential application in clinical and laboratory testing due to its high sensitivity and good stability. The mechanistic studies on the fluorescence enhancement in this system is useful for the understanding of the properties of protein/dye interactions and may be applied to future questions related to fluorescence imaging in cells.

## Acknowledgments

This work is supported by Natural Science Foundation of China (20833010) and Natural Science Foundation of Shandong Province (Z2008B04). The authors thank Dr. J. David Van Horn (Visiting Professor, Shandong University) for editorial assistance.

## References

[1] O.H. Lowry, N.J. Rosebrough, A.L. Farr, R.J. Randall, J. Biol. Chem. 193 (1951) 265.
[2] M.M. Bradford, Anal. Biochem. 72 (1976) 248.
[3] K. Ohsawa, N. Ebata, Anal. Biochem. 135 (1983) 409.
[4] H.Y. Hsieh, P.C. Wang, C.L. Wu, C.W. Huang, C.C. Chieng, F.G. Tsing, Anal. Chem. 81 (2009) 7908.
[5] A.Q. Gong, X.S. Zhu, Y.Y. Hu, S.H. Yu, Talanta 73 (2007) 668.
[6] Y.X. Ci, L. Chen, Analyst 113 (1988) 679.
[7] N. Li, K.A. Li, S.Y. Tong, Anal. Biochem. 233 (1996) 151.
[8] D.H. Li, H.H. Yang, H. Zheng, B. Chen, Q.Y. Chen, J.G. Xu, Chin. J. Anal. Chem. 27 (1999) 1018.
[9] W.W. Qin, Y.J. Bao, G.Q. Gong, S.F. Wu, J.L. Liu, Chin. J. Anal. Chem. 28 (2000) 526.
[10] S.H. Lee, J.K. Suh, M. Li, Bull. Korean Chem. Soc. 24 (2003) 45.
[11] C. Wang, Q. Ma, W.C. Dou, S. Kanwal, G.N. Wang, P.F. Yuan, X.G. Su, Talanta 77 (2009) 1358.
[12] C.Q. Jiang, L. Luo, Anal. Chim. Acta 506 (2004) 171.
[13] C.Q. Ma, K.A. Li, S.Y. Tong, Anal. Chim. Acta 333 (1996) 83.
[14] W.W. Qin, G.Q. Gong, Y.M. Song, Spectrochim. Acta A 56 (2000) 1021.
[15] H. Zhong, J.J. Xu, H.Y. Chen, Talanta 67 (2005) 749.
[16] C.X. Sun, J.H. Yang, L. Li, X. Wu, Y. Liu, S.F. Liu, J. Chromatogr. B 803 (2004) 173.
[17] Y.B. Wang, J.H. Yang, X. Wu, L. Li, S.N. Sun, B.Y. Su, Anal. Lett. 36 (2003) 2063.
[18] J.M. Luan, X.D. Zhang, Chem. Anal. Part B 42 (2006) 687.
[19] A.P. Wei, D.K. Blumenthal, J.N. Herron, Anal. Chem. 66 (1994) 1500.
[20] T. Imasaka, T. Fuchigami, N. Ishibashi, Anal. Sci. 7 (1991) 491.
[21] H. Zhu, C.L. Tong, Anal. Chim. Acta 587 (2007) 187.
[22] P.G. Yi, J.F. Liu, Z.c. Shang, Q.S. Yu, Spectrosc. Spectral Anal. 21 (2001) 826.
[23] M.K. Bahng, C. Mukarakate, D.J. Robichaudand, M.R. Nimlos, Anal. Chim. Acta 651 (2009) 117.
[24] G.C. Zhao, J.J. Zhu, H.Y. Chen, Spectrochim. Acta A 55 (1999) 1109.
[25] X.Z. Feng, Z. Lin, L.J. Yang, C. Wang, C.L. Bai, Talanta 47 (1998) 1223.
[26] S.G. Chen, Y.S. Jiang, R. Lu, W.S. Yang, J.H. Yang, T.J. Li, Z.L. Du, Chem. J. Chin. Univ. 22 (2001) 245.
[27] W.S. Yang, Y.S. Jiang, X.D. Cai, T.J. Li, Sci. China: Ser. B 31 (2001) 161.
[28] H.S. Franks, M.W. Evans, J. Chem. Phys. 13 (1945) 507.
[29] Q.E. Cao, Y.K. Zhao, X.J. Yao, Z.D. Hu, Q.H. Xu, Spectrochim. Acta A 56 (2000) 1319.
[30] M.R. David, D.H. Jonathan, Chirality 16 (2004) 234.
[31] H.E. Edwards, J.K. Thomas, Carbohydr. Res. 65 (1978) 173.
[32] A. Nakajima, Spectrochim. Acta A 39 (1983) 913.
[33] F.G. Sánchez, A.N. Díaz, M.M.L. Guerrero, Anal. Chim. Acta 582 (2007) 92.